Transport coefficients of off-lattice mesoscale-hydrodynamics simulation techniques

Hiroshi Noguchi* and Gerhard Gompper†
Institut für Festkörperforschung, Forschungszentrum Jülich, D-52425 Jülich, Germany
(Received 14 April 2008; published 25 July 2008)

The viscosity and self-diffusion constant of particle-based mesoscale hydrodynamic methods, multiparticle collision dynamics (MPC), and dissipative particle dynamics, are investigated, both with and without angular-momentum conservation. Analytical results are derived for fluids with an ideal-gas equation of state and a finite-time-step dynamics, and compared with simulation data. In particular, the viscosity is derived in a general form for all variants of the MPC method. In general, very good agreement between theory and simulations is obtained.

DOI: 10.1103/PhysRevE.78.016706 PACS number(s): 02.70.−c, 47.11.−j, 66.20.−d

I. INTRODUCTION

Soft matter systems such as polymer solutions, colloidal suspensions, membranes, and microemulsions exhibit many interesting dynamical behaviors, where hydrodynamic flow plays an important role, as do thermal fluctuations. The characteristic time and length scales of soft-matter systems are in the range from nanoseconds to seconds and from nano-to micrometers, respectively, and are thus typically much larger than the atomistic scales. Mesoscale simulation techniques are therefore necessary to simulate these systems for sufficiently large system sizes with reasonable computational effort. Several mesoscale techniques for the simulation of the flow of complex fluids accompanied by thermal fluctuations have been developed in the last decades, such as direct simulation Monte Carlo (DSMC) [1,2], the lattice Boltzmann method [3,4], dissipative particle dynamics (DPD) [5–21], and multiparticle collision dynamics (MPC) [22–44]. DSMC, DPD, and MPC are off-lattice hydrodynamics methods and share many properties. DPD and MPC have been applied to various soft-matter systems such as colloids [15,31–33], polymers [4,6,16,17,34–36], and surfactants [18,19,37–40].

The key features to distinguish DPD and MPC are the application of a Langevin thermostat to the relative velocities of particle pairs or multiparticle collisions, and whether or not to employ collision cells. To understand and elucidate the relation between DPD and MPC, two intermediate methods have been proposed in Ref. [20], which are DPD with a multibody thermostat (DPD-MT) and MPC-Langevin dynamics (MPC-LD). The standard MPC algorithm does not conserve angular momentum. However, an angular-momentum-conserving version of MPC has also been proposed in Ref. [20]. We denote the versions of a simulation method with or without angular-momentum conservation by an extension "+a" or "−a," respectively. The importance of angular-momentum conservation in MPC fluids has been studied in Ref. [43]. In the absence of angular-momentum conservation, an additional torque appears which depends linearly on the vorticity, whereas the velocity field is unaffected. Therefore it is essential to employ +a techniques to simulate systems such as rotating colloids and binary fluids with different viscosities.

In this paper, we investigate the viscosity η and self-diffusion constant D of MPC and DPD methods. The transport coefficients of −a versions of MPC were previously derived analytically, and show good agreement with numerical results [20,26–30]. We derive here analytically the viscosity and diffusion constant of all +a versions of MPC.

The transport coefficients of original version of DPD were derived analytically for systems with an ideal-gas equation of state in the small-time-step limit [12] and with finite time step [21], and phenomenologically for soft-repulsive interactions [21]. Here, we investigate the transport coefficients of DPD-a and DPD-MT for the ideal-gas equation of state with finite time step. The viscosity and diffusion constant are also determined from simulations of simple shear flow with Lees-Edwards boundary conditions and of the mean square displacement of a particle, respectively.

The outline of this paper is as follows. In Sec. II, we describe several versions of MPC, both with and without angular momentum conservation, and calculate their transport coefficients analytically and numerically. Transport coefficients of several versions of DPD are calculated in Sec. III. In Sec. IV, we discuss the upper limits of the local shear rate for which thermostats in MPC and DPD are capable to provide local-equilibrium condition.

II. MULTIPARTICLE COLLISION DYNAMICS (MPC)

A. Simulation method

1. MPC without angular-momentum conservation

MPC is a modification of DSMC to include multiparticle collisions, in order to make the algorithm more efficient in its application [22]. A fluid is described by pointlike particles of mass m. The MPC algorithm consists of alternating streaming and collision steps. In the streaming step, the particles move ballistically,

$$\mathbf{r}_i(t+\Delta t) = \mathbf{r}_i(t) + \mathbf{v}_i \Delta t, \tag{1}$$

where Δt is the time interval between collisions. In the collision step, the particles are sorted into cubic cells of lattice

*Permanent address: Institute for Solid State Physics, University of Tokyo, Japan. noguchi@issp.u-tokyo.ac.jp
†g.gompper@fz-juelich.de

TABLE I. Correlation factors $A=1-\langle v_\alpha \mathbf{\Omega}[\mathbf{v}]_\alpha\rangle/\langle v_\alpha^2\rangle$ and $B=1-\langle \mathbf{\Omega}[\mathbf{v}]_\alpha \mathbf{\Omega}[\mathbf{v}]_\beta\rangle/\langle v_\alpha v_\beta\rangle$ of various MPC methods, where $\alpha,\beta \in \{x,y,z\}$ and $\alpha \neq \beta$.

	A	B	
MPC-SR	$\frac{2}{d}(1-\cos\theta)$	$1-\cos 2\theta$	$(d=2)$
		$\frac{2}{5}(2-\cos\theta-\cos 2\theta)$	$(d=3)$
MPC-RA	$\frac{2}{d}(1-\frac{\sin\theta_0}{\theta_0})$	$1-\frac{\sin 2\theta_0}{2\theta_0}$	$(d=2)$
		$\frac{2}{5}(2-\frac{\sin\theta_0}{\theta_0}-\frac{\sin 2\theta_0}{2\theta_0})$	$(d=3)$
MPC-AT	1	1	
MPC-LD	$\frac{\gamma\Delta t/m}{1+\gamma\Delta t/2m}$	$\frac{2\gamma\Delta t/m}{(1+\gamma\Delta t/2m)^2}$	

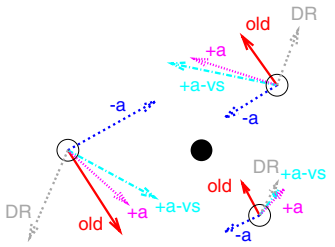

FIG. 1. (Color online) Schematic representation of the collision operation for MPC-SR $\pm a$ and MPC-DR in two-dimensional (2D) space in the co-moving reference frame (with $\Sigma \mathbf{v}_i=0$) at $N_c=3$ and $\theta=\pi/2$. Circles represent the positions of particles (○) and the center of mass (●). "old" indicates the velocities before the collision, "±a" and "DR" represent the velocities after the collision for MPC-SR $\pm a$ and MPC-DR, respectively, and "+a-vs" indicates the velocities after the "+a" collision without velocity rescaling.

constant l_c. The collision procedure is different for each version of MPC. For MPC-a, it is generally given by

$$\mathbf{v}_i^{\text{new}} = \mathbf{v}_c^G + \mathbf{\Omega}[\mathbf{v}_{i,c}], \tag{2}$$

where $\mathbf{v}_c^G$ is the velocity of the center of mass of all particles in the box, and $\mathbf{v}_{i,c}=\mathbf{v}_i-\mathbf{v}_c^G$. The collision operator $\mathbf{\Omega}[\mathbf{v}_{i,c}]$ stochastically changes the relative velocity $\mathbf{v}_{i,c}$, with $\Sigma_{i\in\text{cell}}\mathbf{\Omega}[\mathbf{v}_{i,c}]=0$ to keep the translational momentum constant. This stochastic process is independent for each cell and each time step, and the collision operator $\mathbf{\Omega}[\mathbf{v}_{i,c}]$ depends on whether a particle is inside a cell, but not on its position $\mathbf{r}_i$ within the cell. To guarantee isotropy, the operator must be symmetric on average, with $\langle v_\alpha \mathbf{\Omega}[\mathbf{v}]_\beta\rangle=(1-A)\langle v_\alpha^2\rangle\delta_{\alpha\beta}$, where the subscripts $\alpha,\beta\in\{x,y,z\}$ indicate the spatial components. The constants A and $B=1-\langle \mathbf{\Omega}[\mathbf{v}]_\alpha \mathbf{\Omega}[\mathbf{v}]_\beta\rangle/\langle v_\alpha v_\beta\rangle$ are characteristic quantities of each version (see Table I), which play an essential role in determining the transport coefficients. The operator $\mathbf{\Omega}[\mathbf{v}_{i,c}]$ conserves the total kinetic energy in each cell (local microcanonical ensemble) or is coupled to a thermostat (local canonical ensemble). The collision cells are randomly shifted before each collision step to ensure Galilean invariance [23].

The operator $\mathbf{\Omega}[\mathbf{v}]$ of the original version of MPC is the rotation operator. It is represented by a matrix $\mathbf{\Omega}_R(\mathbf{v})$ which rotates velocities by an angle θ. The rotation axis is chosen randomly for each cell, which requires one integer or two real random numbers in two-(2D) or three-dimensional (3D) space, respectively. In two dimensions, the axis is the $\pm z$ direction (out of plane), i.e., the rotation is clockwise or anticlockwise with the angle θ (see Fig. 1). This original version of MPC is typically denoted MPC or stochastic rotation dynamics (SRD). We denote it MPC-SR-a in this paper, in order to distinguish this particular version clearly from the whole family of MPC techniques. In MPC-SR-a, the energy in each cell is conserved. Under flow conditions, the temperature can be controlled by an additional rescaling of the relative velocities $\mathbf{v}_{i,c}\to\mathbf{v}_{i,c}\sqrt{d(N-N_{\text{cell}})k_BT/m\Sigma_i\mathbf{v}_{i,c}^2}$, where d is the spatial dimension, N is the total number of particles, and N_{cell} is the number of cells occupied by particles. This corresponds to a velocity-scaling version of the profile-unbiased thermostat (PUT) [45], where cells are introduced to thermostat local velocities relative to the center-of-mass velocity of each cell. The number $d(N-N_{\text{cell}})$ of the degrees of freedom should be sufficiently large for the central-limit theorem to apply. This usually implies that the number of cells included in the calculation of the rescaling factor is large. When the velocity rescaling is performed on the level of single collision cells, the Monte Carlo scheme proposed in Ref. [33] should be employed.

In the random angle version of MPC (denoted MPC-RA-a) [25], the same matrix $\mathbf{\Omega}_R(\mathbf{v})$ is employed, but the rotational angle θ is also selected stochastically varied in the interval $0\leqslant\theta<\theta_0$. In MPC-RA-$a$, one or three real random numbers are required for each cell in two or three dimensions, respectively.

In the Andersen-thermostat [46,47] version of MPC, denoted MPC-AT [20,25], the operator completely renews the relative velocities in the cell, $\mathbf{\Omega}[\mathbf{v}]=\mathbf{v}_i^{\text{ran}}-\Sigma_{j\in\text{cell}}\mathbf{v}_j^{\text{ran}}/N_c$, where N_c is the number of particles in a cell. A velocity $\mathbf{v}_i^{\text{ran}}$ is chosen from a Maxwell-Boltzmann distribution. Thus, in MPC-AT-a, the velocities of particles are updated by

$$\mathbf{v}_i^{\text{new}} = \mathbf{v}_c^G + \mathbf{v}_i^{\text{ran}} - \sum_{j\in\text{cell}} \frac{\mathbf{v}_j^{\text{ran}}}{N_c}. \tag{3}$$

Instead of the energy, the temperature is constant in MPC-AT.

In the Langevin version of MPC (MPC-LD-a) [20], the Langevin thermostat is applied to the relative velocities in a collision cell. The particle motion is given by

$$m\frac{d\mathbf{v}_i}{dt} = -\frac{\partial U}{\partial \mathbf{r}_i} - \gamma\mathbf{v}_{i,c} + \sqrt{\gamma}\left\{\boldsymbol{\xi}_i(t) - \sum_{j\in\text{cell}}\frac{\boldsymbol{\xi}_j(t)}{N_c}\right\}. \tag{4}$$

In order to satisfy the fluctuation-dissipation theorem, the Gaussian white noise $\boldsymbol{\xi}_i(t)$ has to have the average $\langle\xi_{i,\alpha}(t)\rangle=0$ and the variance $\langle\xi_{i,\alpha}(t)\xi_{j,\beta}(t')\rangle=2k_BT\delta_{ij}\delta_{\alpha\beta}\delta(t-t')$, where $\alpha,\beta\in\{x,y,z\}$ and k_BT is the thermal energy. We consider in this paper only fluids with an ideal-gas equation state, i.e., $U\equiv 0$ in Eq. (4). The finite time-step version of MPC-LD-a is given by the leapfrog algorithm,

$$\mathbf{r}_i(t_{n+1/2}) = \mathbf{r}_i(t_{n-1/2}) + \mathbf{v}_{i,n}\Delta t, \tag{5}$$

$$\mathbf{v}_i(t_{n+1}) = \mathbf{v}_c^G + a_{ld}\mathbf{v}_{i,c}(t_n) + b_{ld}\left\{\boldsymbol{\xi}_{i,n} - \sum_{j\in\text{cell}} \frac{\boldsymbol{\xi}_{j,n}}{N_c}\right\},$$

$$\text{with } a_{ld} = \frac{1-\gamma\Delta t/2m}{1+\gamma\Delta t/2m}, \quad b_{ld} = \frac{\sqrt{\gamma\Delta t}/m}{1+\gamma\Delta t/2m}, \tag{6}$$

where $\langle\xi_{i,n,\alpha}\rangle=0$ and $\langle\xi_{i,n,\alpha}\xi_{j,n',\beta}\rangle=2k_BT\delta_{ij}\delta_{\alpha\beta}\delta_{nn'}$. Thus, the collision operator is $\mathbf{\Omega}[\mathbf{v}_{i,c}]=a_{ld}\mathbf{v}_{i,c}+b_{ld}\{\boldsymbol{\xi}_{i,n}-\Sigma\boldsymbol{\xi}_{j,n}/N_c\}$. MPC-LD with $\gamma\Delta t/2m=1$ coincides with MPC-AT.

MPC-AT and MPC-LD can suppress temperature gradient better than MPC-SR and MPC-RA, since their thermostats are local and more efficient. In MPC-AT and MPC-LD, the correlations have a simple relation, $(1-B)=(1-A)^2$. However, MPC-SR and MPC-RA have additional correlations between x and y components, i.e., $(1-B)\neq(1-A)^2$ as shown in Table I.

2. MPC with angular-momentum conservation

Collisions described by Eq. (2) conserve translational momentum, but do *not* conserve angular momentum. However, angular-momentum conservation can be imposed by an additional constraint. This modification is straightforward for the MPC versions with an intrinsic thermostat (such as MPC-AT and MPC-LD). In this case, the collision is given by

$$\mathbf{v}_i^{new} = \mathbf{v}_c^G + \mathbf{\Omega}[\mathbf{v}_{i,c}] + m\mathbf{\Pi}^{-1} \times \sum_{j\in\text{cell}} \{\mathbf{r}_{j,c}\times(\mathbf{v}_{j,c}-\mathbf{\Omega}[\mathbf{v}_{j,c}])\}\times\mathbf{r}_{i,c}, \tag{7}$$

where $\mathbf{\Pi}$ is the moment-of-inertia tensor of the particles in the cell. The relative position is $\mathbf{r}_{i,c}=\mathbf{r}_i-\mathbf{r}_c^G$ where $\mathbf{r}_c^G$ is the center of mass of the particles in the cell. The angular momentum of the cell after the collision, $\mathbf{\Pi}\omega_c=m\Sigma\mathbf{r}_{j,c}\times\mathbf{v}_{j,c}$, is the same as before the collision. The subtraction of either position or velocity of the center of mass can be omitted in the last term of Eq. (7), since $\Sigma\mathbf{r}_{j,c}\times\mathbf{v}_{j,c}=\Sigma\mathbf{r}_j\times\mathbf{v}_{j,c}=\Sigma\mathbf{r}_{j,c}\times\mathbf{v}_j$.

For MPC-AT+a or MPC-LD+a, the terms

$$\mathbf{f}_{AT+a} = m\mathbf{\Pi}^{-1}\sum_{j\in\text{cell}}\{\mathbf{r}_{j,c}\times(\mathbf{v}_j-\mathbf{v}_j^{ran})\}\times\mathbf{r}_{i,c}, \tag{8}$$

$$\mathbf{f}_{LD+a} = m\mathbf{\Pi}^{-1}\sum_{j\in\text{cell}}\{\mathbf{r}_{j,c}\times\{\gamma\mathbf{v}_j-\sqrt{\gamma}\boldsymbol{\xi}_j(t)\}\}\times\mathbf{r}_{i,c} \tag{9}$$

are added to Eqs. (3) and (4), respectively [20].

When Eq. (7) is applied to the operator of MPC-SR or MPC-RA, the kinetic energy is *not* conserved. Thus the collision process has to be modified by combining it with velocity rescaling to conserve the energy,

$$\mathbf{v}_i^{new} = \mathbf{v}_c^G + m\mathbf{\Pi}^{-1}\sum_{j\in\text{cell}}(\mathbf{r}_{j,c}\times\mathbf{v}_{j,c})\times\mathbf{r}_{i,c} + \phi\left\{\mathbf{\Omega}[\mathbf{v}_{i,c}] - m\mathbf{\Pi}^{-1}\sum_{j\in\text{cell}}(\mathbf{r}_{j,c}\times\mathbf{\Omega}[\mathbf{v}_{j,c}])\times\mathbf{r}_{i,c}\right\}, \tag{10}$$

where $\phi=\{\Sigma_{j\in\text{cell}}(\mathbf{u}_j^{old})^2\}/\{\Sigma_{j\in\text{cell}}(\mathbf{u}_j^{\Omega})^2\}$. Here, the relative velocities before and after the collision, $\mathbf{u}_j^{old}$ and $\mathbf{u}_j^{\Omega}$, respectively, are given by $\mathbf{u}_i=\mathbf{v}_{i,c}-m\mathbf{\Pi}^{-1}\Sigma_{j\in\text{cell}}(\mathbf{r}_{j,c}\times\mathbf{v}_{j,c})\times\mathbf{r}_{i,c}$, where the total translational and angular velocities of the cell are subtracted. This collision is shown schematically in Fig. 1. Under the molecular-chaos assumption, this yields the ideal-gas equation of state. However, the molecular-chaos assumption is not perfectly valid. Thus the radial distribution function $g(r)$ of MPC-SR+a exhibits deviations from the uniform distribution of the ideal gas, in particular for small n or small Δt (see Fig. 2). Note that small time steps Δt are essential to model fluids with high Schmidt numbers and low Reynolds numbers [34]. If the velocity rescaling for the energy conservation is done not for each cell but for the sum of many cells, this deviation becomes larger. A similar deviation is seen in DPD simulations [8] with the modified velocity-Verlet algorithm [6]. These deviations arise due to the lack of time-reversal symmetry. The collision operators of MPC-AT+a and MPC-LD+a and all $-a$ versions of MPC have time-reversal symmetry and give the correct uniform $g(r)$—see, e.g., the data of MPC-AT+a in Fig. 2. Thus MPC-SR+a should not be used for small n or small Δt. We recommend to check $g(r)$ for any new MPC operator.

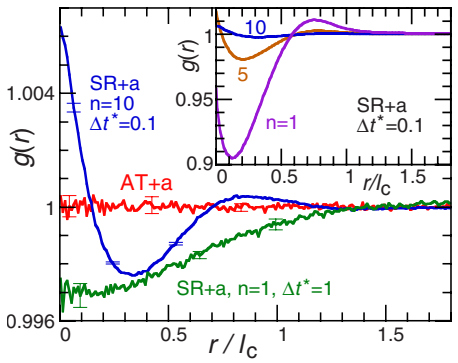

FIG. 2. (Color online) Radial distribution function $g(r)$ of MPC-SR+a (with $n=1$, $\Delta t^*=1$ and $n=10$, $\Delta t^*=0.1$) and MPC-AT+a (with $n=1$, $\Delta t^*=0.1$) in two dimensions. The inset shows the n dependence of $g(r)$ of MPC-SR+a at $\Delta t^*=0.1$. Error bars are shown at several data points.

An alternative modification of MPC-SR for *two-dimensional* fluids to conserve angular momentum has been proposed recently by Ryder [48] (see also Ref. [44]). We denote this algorithm MPC-DR (deterministic rotation). In MPC-DR, a rotational angle is chosen deterministically to keep the total angular momentum of particles in a collision cell constant by the requirement $W\{1-\cos(\theta)\}+Q\sin(\theta)=0$, where $W=\Sigma_{j\in\text{cell}}\mathbf{r}_{j,c}\times\mathbf{v}_{j,c}$ and $Q=\Sigma_{j\in\text{cell}}\mathbf{r}_{j,c}\cdot\mathbf{v}_{j,c}$. This implies

$$\cos(\theta)=\frac{W^2-Q^2}{W^2+Q^2} \text{ and } \sin(\theta)=-\frac{2WQ}{W^2+Q^2}. \tag{11}$$

The velocities after a collision in MPC-DR are different from those in MPC-SR+a, since the $+a$ procedure (from $-a$ to $+a$-vs in Fig. 1) does not change the radial velocities. MPC-DR gives the correct uniform $g(r)$ and is less time consuming than other $+a$ versions of MPC. We also checked that MPC-DR yields the correct constant angular velocities for phase-separated binary fluids with different viscosities in

a circular Couette flow, as described in Sec. IV C of Ref. [43]. However, this algorithm cannot be generalized to three-dimensional systems.

B. Transport coefficients

1. Stress tensor

Angular-momentum conservation implies that the stress tensor $\sigma_{\alpha\beta}$ for an isotropic Newtonian fluid is symmetric, i.e., $\sigma_{\alpha\beta}=\sigma_{\beta\alpha}$ [49]. In contrast, MPC$-a$ fluids have an asymmetric stress tensor

$$\sigma_{\alpha\beta}=\lambda(\nabla\cdot\mathbf{v})\delta_{\alpha\beta}+\bar{\eta}\left(\frac{\partial v_\alpha}{\partial x_\beta}+\frac{\partial v_\beta}{\partial x_\alpha}\right)+\check{\eta}\left(\frac{\partial v_\alpha}{\partial x_\beta}-\frac{\partial v_\beta}{\partial x_\alpha}\right), \tag{12}$$

because of the lack of angular-momentum conservation [27,29,43], where $\alpha,\beta\in\{x,y,z\}$ and λ is the second viscosity coefficient. $\bar{\eta}$ and $\check{\eta}$ are the symmetric and antisymmetric components of the viscosity, respectively. The last term in Eq. (12) implies that the stress depends linearly on the vorticity $\nabla\times\mathbf{v}$, and does not conserve angular momentum. Thus this term vanishes (i.e., $\check{\eta}=0$) in angular-momentum conserving systems.

The evolution of the velocity field $\mathbf{v}(\mathbf{r})$ is determined by

$$\rho\frac{D\mathbf{v}}{Dt}=-\nabla P+(\lambda+\bar{\eta}-\eta)\nabla(\nabla\cdot\mathbf{v})+(\bar{\eta}+\check{\eta})\nabla^2\mathbf{v}, \tag{13}$$

where D/Dt is Lagrange's derivative and P is the pressure field. When a fluid is incompressible, Eq. (13) is the normal Navier-Stokes equation with viscosity $\eta=\bar{\eta}+\check{\eta}$. This is consistent with the usual definition of the shear viscosity $\eta=\sigma_{xy}/\dot{\gamma}$ in simple shear flow with velocity field $\mathbf{v}=\dot{\gamma}y\mathbf{e}_x$, where $\mathbf{e}_x$ is the unit vector along the x direction. Since both the equations of continuity and of velocity evolution are of the same forms in systems with and without angular-momentum conservation, the absence of angular-momentum conservation does not affect the velocity field of a fluid when the boundary conditions are given by velocities. However, it generates an additional torque, as described in detail in Ref. [43]. In this paper, we discuss the stress tensor of various MPC and DPD methods.

2. MPC without angular-momentum conservation

The shear viscosity is calculated from $\sigma_{xy}/\dot{\gamma}=\eta=\bar{\eta}+\check{\eta}$ in simple shear flow with $\mathbf{v}=\dot{\gamma}y\mathbf{e}_x$. The viscosity of MPC fluids consists of two contributions, $\eta=\eta_{\rm kin}+\eta_{\rm col}$, where the kinetic viscosity $\eta_{\rm kin}$ and the collisional viscosity $\eta_{\rm col}$ result from the momentum transfer due to particle displacements and collisions, respectively. The derivation of the viscosity for MPC-SR$-a$ described in Refs. [26–30] can be employed directly for other $-a$ versions of MPC, since the differences appear only in the factors A and B listed in Table I.

The kinetic stress $\sigma_{xy}^{\rm kin}=\eta_{\rm kin}\dot{\gamma}$ is the momentum flux due to particles crossing a xz plane at $y=y_0=0$. The stress due to streaming in the time interval $[t,t+\Delta t]$ is written as

$$\sigma_{xy}^{\rm kin}=\frac{m}{S\Delta t}\left\langle\sum_{y_i(t)>0,v_{i,y}<-y_i(t)/\Delta t}v_{i,x}-\sum_{y_i(t)<0,v_{i,y}>-y_i(t)/\Delta t}v_{i,x}\right\rangle, \tag{14}$$

where S is the surface area of the considered plane. The average over equivalent xz planes yields

$$\sigma_{xy}^{\rm kin}=-mn\langle v_xv_y\rangle_{t+\Delta t/2}=-\frac{m}{V}\sum_i\langle v_{i,x}v_{i,y}\rangle, \tag{15}$$

where $n=\langle N_{\rm c}\rangle$ is the average number of particles per cell, and V is the volume of the considered region $\mathcal{V}$, with $\mathbf{r}_i\in\mathcal{V}$; here the middle position $\mathbf{r}_i(t+\Delta t/2)=\mathbf{r}_i(t)+\mathbf{v}_i\Delta t/2$ during streaming is employed to determine whether the ith particle is inside the region $\mathcal{V}$. The expression (15) is symmetric in x and y. The symmetry of the kinetic part of the stress tensor, i.e., $\sigma_{yx}^{\rm kin}=\sigma_{xy}^{\rm kin}$, implies $\eta_{\rm kin}=0$ for all versions of MPC and DPD. Numerically, $\sigma_{xy}^{\rm kin}$ and $\eta_{\rm kin}$ can be calculated from Eqs. (14) or (15). The velocity distribution is shifted by particle streaming so that

$$\begin{aligned}\langle v_xv_y\rangle_{t,t+\Delta t}&=\int d\mathbf{v}v_xv_yP_v(\mathbf{v}\mp\dot{\gamma}v_y\Delta t\mathbf{e}_x/2)\\&=\langle v_xv_y\rangle_{t+\Delta t/2}\pm\langle v_y^2\rangle\dot{\gamma}\Delta t/2,\end{aligned} \tag{16}$$

where $P_v(\mathbf{v})$ is the velocity probability distribution. The velocity distribution is modified by the MPC collisions so that $\langle v_x^{\rm new}v_y^{\rm new}\rangle=(1-c_{\rm m})\langle v_xv_y\rangle$, where the factor $c_{\rm m}$ is determined later. The self-consistency condition of a stationary shear flow is $\langle v_xv_y\rangle_t=\langle v_xv_y\rangle_{t+\Delta t}=(1-c_{\rm m})(\langle v_xv_y\rangle_t-\dot{\gamma}\Delta t\langle v_y^2\rangle)$. The kinetic viscosity $\eta_{\rm kin}$ is then given by [26]

$$\eta_{\rm kin}=\frac{nk_{\rm B}T\Delta t}{l_{\rm c}^d}\left(\frac{1}{c_{\rm m}}-\frac{1}{2}\right). \tag{17}$$

Equation (17) holds for all $\pm a$ versions of MPC and DPD.

The velocity correlations for MPC$-a$ are calculated by using Eq. (2),

$$\begin{aligned}\langle v_{i,x}^{\rm new}v_{i,y}^{\rm new}\rangle&=\left\{\frac{1}{N_{\rm c}^2}+\frac{2}{N_{\rm c}}\left(1-\frac{1}{N_{\rm c}}\right)(1-A)+\left(1-\frac{1}{N_{\rm c}}\right)^2(1-B)\right\}\\&\quad\times\langle v_{i,x}v_{i,y}\rangle+\frac{2A-B}{N_{\rm c}^2}\sum_{j\neq i}\langle v_{j,x}v_{j,y}\rangle\\&=\left\{1-B\left(1-\frac{1}{N_{\rm c}}\right)\right\}\langle v_{i,x}v_{i,y}\rangle,\end{aligned} \tag{18}$$

where molecular chaos is assumed, i.e., $\langle v_{i,x}v_{i,y}\rangle=\langle v_{j,x}v_{j,y}\rangle$ and $\langle v_{i,x}v_{j,y}\rangle=0$ for $i\neq j$. Thus the correlation factor for a cell occupied by $N_{\rm c}$ particles is $c(N_{\rm c})=B(1-1/N_{\rm c})$. An MPC fluid is thermodynamically an ideal gas, so that the cell occupation number $N_{\rm c}$ fluctuates with the Poisson distribution, $P(N_{\rm c})=e^{-n}n^{N_{\rm c}}/N_{\rm c}!$ with $n=\langle N_{\rm c}\rangle$. Thus the average correlation is given by $c_{\rm m}=\sum_{k=1}^{\infty}c(k)P(k)k/n=B(n-1+e^{-n})/n$. The kinetic viscosity of MPC$-a$ is then given by

$$\eta_{\rm kin}=\frac{nk_{\rm B}T\Delta t}{l_{\rm c}^d}\left\{\frac{n/B}{n-1+e^{-n}}-\frac{1}{2}\right\}. \tag{19}$$

The collisional stress $\sigma_{xy}^{\mathrm{col}}=\eta_{\mathrm{col}}\dot{\gamma}$ is the momentum flux due to MPC collisions in cells crossing a plane at $y=y_0$. It is given by [26]

$$\sigma_{xy}^{\mathrm{col}}=-\frac{m}{l_{\mathrm{c}}^{d-1}\Delta t}\sum_{y_0<y_i,i\in\mathrm{cell}}\langle v_{i,x}^{\mathrm{new}}-v_{i,x}\rangle. \tag{20}$$

When Eq. (20) is averaged over the planes crossing the cell, $y_{\mathrm{cc}}-l_{\mathrm{c}}/2<y_0<y_{\mathrm{cc}}+l_{\mathrm{c}}/2$, the stress reads

$$\sigma_{xy}^{\mathrm{col}}=-\frac{m}{l_{\mathrm{c}}^{d-1}\Delta t}\sum_{i\in\mathrm{cell}}\left(\frac{y_{i,\mathrm{cc}}}{l_{\mathrm{c}}}+\frac{1}{2}\right)\langle v_{i,x}^{\mathrm{new}}-v_{i,x}\rangle, \tag{21}$$

where $y_{i,\mathrm{cc}}=y_i-y_{\mathrm{cc}}$ and y_{cc} is the y component of the center-of-cell position $\mathbf{r}_{\mathrm{cc}}$. Numerically, $\sigma_{xy}^{\mathrm{col}}$ and η_{col} can be calculated from either Eqs. (20) or (21). The mean velocity difference is $\langle v_{i,x}^{\mathrm{new}}-v_{i,x}\rangle=-(1-\frac{1}{N_{\mathrm{c}}})A\dot{\gamma}y_{i,\mathrm{cc}}$, because $\langle\mathbf{v}_{\mathrm{c}}^{\mathrm{G}}\rangle=\mathbf{v}_i/N_{\mathrm{c}}$, where y_j is averaged over $-l_{\mathrm{c}}/2<y_j<l_{\mathrm{c}}/2$ for $j\neq i$ at $y_{\mathrm{cc}}=0$. Then the collisional viscosity η_{col} of MPC$-a$ is given by

$$\eta_{\mathrm{col}}=\frac{Am}{l_{\mathrm{c}}^{d}\Delta t}\left\{\sum_{N_{\mathrm{c}}=1}^{\infty}(N_{\mathrm{c}}-1)P(N_{\mathrm{c}})\right\}\int_{-l_{\mathrm{c}}/2}^{l_{\mathrm{c}}/2}dy\left(\frac{y}{l_{\mathrm{c}}}+\frac{1}{2}\right)y$$
$$=\frac{Am(n-1+e^{-n})}{12l_{\mathrm{c}}^{d-2}\Delta t}. \tag{22}$$

The vorticity viscosity $\check{\eta}_{\mathrm{col}}\dot{\gamma}=\sigma_{xy}^{\mathrm{col}}-\sigma_{yx}^{\mathrm{col}}$ is proportional to the angular-momentum transfer with respect to the origin $(x_{\mathrm{cc}}-l_{\mathrm{c}}/2,y_{\mathrm{cc}}-l_{\mathrm{c}}/2)$; see Eq. (21). Thus the vorticity viscosity of MPC$+a$ vanishes, $\check{\eta}_{\mathrm{col}}=0$, because of angular-momentum conservation. For MPC$-a$, the molecular-chaos assumption gives $\sigma_{yx}^{\mathrm{col}}=0$, because $\langle v_y^{\mathrm{new}}(x)\rangle=\langle v_y(x)\rangle=0$. Thus the viscosities are $\check{\eta}=\bar{\eta}=\eta_{\mathrm{col}}/2$ [27,43]. This relation holds for all $-a$ versions of MPC and DPD described in this paper.

As an extension of this approach, the angular-momentum constraint can be applied only partially, by employing alternatively the MPC-collision algorithms which conserve [given by Eq. (7)] and do not conserve [determined by the difference of the right-hand sides of Eqs. (2) and (7)] angular momentum. In this way, the viscosity ratio $\check{\eta}/\eta$ can be varied continuously between 0 and approximately 1.

Next, we derive the self-diffusion constant D of MPC$-a$. Under the molecular-chaos assumption, the velocity correlation function decays exponentially, $\langle v_{i,x}(k\Delta t)v_{i,x}(0)\rangle=(1-s_{\mathrm{m}})^k k_{\mathrm{B}}T/m$ with $1-s_{\mathrm{m}}=\langle v_{i,x}^{\mathrm{new}}v_{i,x}\rangle/\langle v_{i,x}^2\rangle$. The diffusion constant is given by [28]

$$D=\frac{\Delta t}{2}\left\{\langle v_{i,x}(0)^2\rangle+2\sum_{k=1}^{\infty}\langle v_{i,x}(k\Delta t)v_{i,x}(0)\rangle\right\}$$
$$=\frac{k_{\mathrm{B}}T\Delta t}{m}\left(\frac{1}{s_{\mathrm{m}}}-\frac{1}{2}\right). \tag{23}$$

In MPC$-a$, the correlation factor is $s_{\mathrm{m}}=\sum_{k=1}^{\infty}s(k)P(k)k/n=A(n-1+e^{-n})/n$ with $s(N_{\mathrm{c}})=A(1-1/N_{\mathrm{c}})$; this implies

$$D=\frac{k_{\mathrm{B}}T\Delta t}{m}\left(\frac{n/A}{n-1+e^{-n}}-\frac{1}{2}\right). \tag{24}$$

However, the velocity autocorrelation function $\langle v_x(k\Delta t)v_x(0)\rangle$ for small mean free path $l_\lambda=\Delta t\sqrt{k_{\mathrm{B}}T/m_0}$ has a long-time tail due to hydrodynamic backflow [28,32,34]. This leads to an additional hydrodynamic contribution to the diffusion constant D, which thereby becomes larger than predicted by Eq. (25).

3. MPC with angular-momentum conservation

To derive expressions for the self-diffusion constant and viscosity of MPC$+a$, we employ Eqs. (17), (21), and (23), which remain valid with angular-momentum conservation. However, the correlation factors s_{m} and c_{m} of MPC$+a$ are different from those of MPC$-a$. First, we consider the limit of large n, where $s_{\mathrm{m}}=s(n)$ and $c_{\mathrm{m}}=c(n)$, and derive the corrections for small n subsequently. The velocity correlation is calculated from $\Sigma_j(\mathbf{r}_{j,\mathrm{c}}\times\mathbf{v}_{j,\mathrm{c}})\times\mathbf{r}_{i,\mathrm{c}}=\Sigma_j(\mathbf{r}_{i,\mathrm{c}}\cdot\mathbf{r}_{j,\mathrm{c}})\mathbf{v}_j-(\mathbf{v}_j\cdot\mathbf{r}_{i,\mathrm{c}})\mathbf{r}_{j,\mathrm{c}}$ with the molecular-chaos assumption. The positions of particles $\mathbf{r}_i$ are averaged over the cell, so that $\mathbf{r}_{i,\mathrm{c}}^2=(1-1/N_{\mathrm{c}})l_{\mathrm{c}}^2d/12$ and $\mathbf{\Pi}=(N_{\mathrm{c}}-1)ml_{\mathrm{c}}^2\mathbf{I}/6$ where $\mathbf{I}$ is the identity matrix. Angular-momentum conservation implies additional correlations, which result in

$$s(N_{\mathrm{c}})=A\left(1-\frac{1}{N_{\mathrm{c}}}\right)-\frac{Ad}{2N_{\mathrm{c}}}(1-\langle\hat{x}_{i,\mathrm{cc}}^2\rangle)=A\left(1-\frac{d+1}{2N_{\mathrm{c}}}\right), \tag{25}$$

where $\hat{x}_{i,\mathrm{cc}}$ is the x component of unit vector $\hat{\mathbf{r}}_{i,\mathrm{cc}}=\mathbf{r}_{i,\mathrm{cc}}/r_{i,\mathrm{cc}}$ and $\langle\hat{x}_{i,\mathrm{cc}}^2\rangle=1/d$. The diffusion constant of MPC$+a$ for large n is thus found to be

$$D=\frac{k_{\mathrm{B}}T\Delta t}{m}\left(\frac{n/A}{n-(d+1)/2}-\frac{1}{2}\right). \tag{26}$$

For the calculation of the kinetic viscosity, we obtain the v_xv_y correlation factor

$$c(N_{\mathrm{c}})=B\left(1-\frac{3d+2}{4N_{\mathrm{c}}}\right)+\frac{Ad}{2N_{\mathrm{c}}}+O(N_{\mathrm{c}}^{-2}). \tag{27}$$

The kinetic viscosity η_{kin} for large n is then given by Eqs. (17) and (27) with $c_{\mathrm{m}}=c(n)$. For MPC-AT$+a$ and MPC-LD$+a$, this implies for large n that

$$\eta_{\mathrm{kin}}^{\mathrm{AT+a}}=\frac{nk_{\mathrm{B}}T\Delta t}{l_{\mathrm{c}}^d}\left\{\frac{n}{n-(d+2)/4}-\frac{1}{2}\right\}, \tag{28}$$

$$\eta_{\mathrm{kin}}^{\mathrm{LD+a}}=\frac{nk_{\mathrm{B}}T}{l_{\mathrm{c}}^d}\left\{\frac{mn(1+\gamma\Delta t/2m)^2/\gamma}{2n-d-1+d\gamma\Delta t/4m}-\frac{\Delta t}{2}\right\}. \tag{29}$$

Note that η and D of MPC-LD$\pm a$ have a different dependence on the time step Δt than other MPC algorithms, since their correlation factors A and B depend on Δt (see Table I).

The mean velocity difference for MPC$+a$ is given by

$$\langle v_{i,x}^{\mathrm{new}}-v_{i,x}\rangle=-\left(1-\frac{1}{N_{\mathrm{c}}}\right)A(\dot{\gamma}-\langle\omega\rangle)y_{i,\mathrm{cc}}. \tag{30}$$

The z component of the velocity is pre-averaged, the angular velocity is in the vorticity direction, $\omega=\omega\mathbf{e}_z$, and $\langle\mathbf{v}_j\rangle=\dot{\gamma}y_{j,\mathrm{cc}}\mathbf{e}_x$, so that

$$\langle\boldsymbol{\omega}\rangle=\left\langle\frac{\Sigma_j\mathbf{r}_{j,\mathrm{c}}\times\mathbf{v}_{j,\mathrm{c}}}{\Sigma_j x_{j,\mathrm{c}}^2+y_{j,\mathrm{c}}^2}\right\rangle,$$

$$\langle\omega\rangle = \frac{y_{i,\mathrm{cc}}^2 + (N_\mathrm{c}-1)l_\mathrm{c}^2/12}{y_{i,\mathrm{cc}}^2 + (2N_\mathrm{c}-1)l_\mathrm{c}^2/12}\dot{\gamma}, \tag{31}$$

where the numerator and denominator are averaged over $x_{i,\mathrm{cc}}$, $x_{j,\mathrm{cc}}$, and $y_{j,\mathrm{cc}}$ independently. When $\langle\omega\rangle$ is also preaveraged over $y_{i,\mathrm{cc}}$, $\langle\omega\rangle=\dot{\gamma}/2$ is obtained. However, Eq. (21), together with Eq. (30) contains an integral with $y_{i,\mathrm{cc}}^2$, which yields an additional correction term of $O(N_\mathrm{c}^{-1})$,

$$\int_{-l_\mathrm{c}/2}^{l_\mathrm{c}/2} \frac{\langle\omega\rangle y_{i,\mathrm{cc}}^2}{\dot{\gamma}l_\mathrm{c}^3} dy_{i,\mathrm{cc}} = \frac{1}{24}\left(1+\frac{2}{5N_\mathrm{c}}\right) + O(N_\mathrm{c}^{-2}). \tag{32}$$

Then, the collisional viscosity η_col of MPC+a for large n is given by

$$\eta_\mathrm{col} = \frac{Am(n-7/5)}{24l_\mathrm{c}^{d-2}\Delta t}. \tag{33}$$

Next, we derive the correction terms for small n. For $N_\mathrm{c}=1$ or 2, Eqs. (25) and (27) do not give the correct correlation factors $s(N_\mathrm{c})$ and $c(N_\mathrm{c})$ for MPC+a—unlike for MPC−a. First, there is no velocity transfer for $N_\mathrm{c}=1$, i.e., $s(1)=c(1)=0$. Second, in the energy-conserving versions (MPC-SR+a and MPC-RA+a), all dN_c degrees of freedom are determined for $N_\mathrm{c}=2$ by the conservation of energy (one degree of freedom), and translational (d degrees) and angular ($d-1$ degrees) momentum, so that $s(2)=c(2)=0$. In the versions with an intrinsic thermostat (MPC-AT+a and MPC-LD+a), one degree of freedom remains for the velocity transfer for $N_\mathrm{c}=2$, so that $s(2)=A/2d$ and $c(2)=(A+B/d)/(d+2)$. Thus $s_\mathrm{m}=\Sigma_{k=3}^{\infty}s(k)P(k)k/n$ for energy-conserving versions of MPC, and $s_\mathrm{m}=P(2)A/dn+\Sigma_{k=3}^{\infty}s(k)P(k)k/n$ for intrinsic-thermostat versions of MPC. For MPC-SR+a and MPC-RA+a, the diffusion constant D, and the viscosities η_kin and η_col are given by Eqs. (23) and (17) with

$$s_\mathrm{m} = A\left\{1-\frac{d+1}{2n}+\frac{e^{-n}}{2}\left(\frac{(d-3)n}{2}+d-1+\frac{d+1}{n}\right)\right\},$$

$$c_\mathrm{m} = B\{1-e^{-n}(1+n)\} + \left\{Ad-\frac{B(3d+2)}{2}\right\}\frac{1-e^{-n}(1+n+n^2/2)}{2n},$$

$$\eta_\mathrm{col} = \frac{Am}{24l_\mathrm{c}^{d-2}\Delta t}\left\{n-\frac{7}{5}+e^{-n}\left(\frac{7}{5}+\frac{2n}{5}-\frac{3n^2}{10}\right)\right\}. \tag{34}$$

For MPC-AT+a and MPC-LD+a, the diffusion constant D and the viscosity contributions η_kin and η_col are given by Eqs. (23) and (17) with

$$s_\mathrm{m} = A\left\{1-\frac{d+1}{2n}+\frac{e^{-n}}{2}\left(\frac{(d-1)(d-2)n}{2d}+d-1+\frac{d+1}{n}\right)\right\}, \tag{35}$$

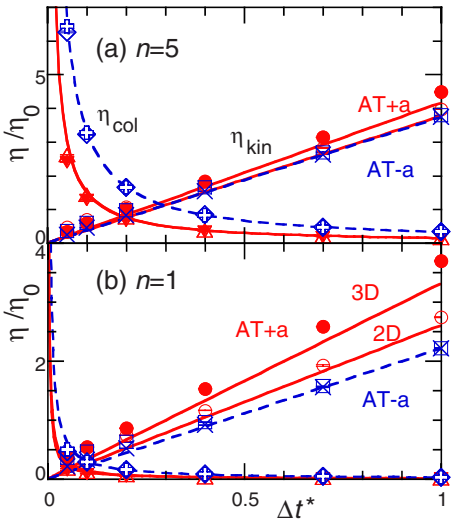

FIG. 3. (Color online) Dependence of the viscosity in MPC-AT$\pm a$ on Δt^* in two-or three-dimensional space for (a) $n=5$ and (b) $n=1$. Symbols represent the numerical data of MPC-AT+a in two dimensions (○, △) or three dimensions (●, ▼) and MPC-AT−a in two dimensions (□, ◇) or three dimensions (×, +), respectively. Solid and dashed lines represent analytical results for MPC-AT+a and MPC-AT−a, respectively. Error bars are smaller than the size of symbols.

$$c_\mathrm{m} = B\{1-e^{-n}(1+n)\} + \left(A+\frac{B}{d}\right)\frac{ne^{-n}}{d+2} + \left\{Ad-\frac{B(3d+2)}{2}\right\}\frac{1-e^{-n}(1+n+n^2/2)}{2n}, \tag{36}$$

$$\eta_\mathrm{col} = \frac{Am}{24l_\mathrm{c}^{d-2}\Delta t}\times\left[n-\frac{7}{5}+e^{-n}\left\{\frac{7}{5}+\frac{2n}{5}+\left(\frac{1}{d}-\frac{3}{10}\right)n^2\right\}\right]. \tag{37}$$

For MPC-DR, the rotation angle θ is uniformly distributed in $-\pi\leqslant\theta<\pi$ under the molecular-chaos assumption. Thus the transport coefficients of MPC-DR coincide with those of MPC-RA+a at $\theta_0=\pi$. Thus the diffusion constant D, and the viscosities η_kin and η_col of MPC-DR are given by Eqs. (23), (17), and (34) with $A=B=1$. Here, the term c_m can be written in a simpler form, $c_\mathrm{m}=\{n-1+e^{-n}(1-n^2/2)\}/n$.

C. Numerical results

Figures 3–6 show the viscosities η_kin and η_col for five MPC methods with or without the angular-momentum conservation. The results are displayed in form of dimensionless quantities with length and time units l_c and $\tau_0=l_\mathrm{c}\sqrt{m/k_\mathrm{B}T}$, respectively. The main parameters which control the properties of MPC fluids, the time step and friction constant, have the dimensionless form $\Delta t^*=\Delta t/\tau_0$ and $\gamma^*=\gamma\tau_0/m$. Similarly, the viscosity and diffusion constant of a particle are shown in units of $\eta_0=\sqrt{mk_\mathrm{B}T}/l_\mathrm{c}^{d-1}$ and $D_0=l_\mathrm{c}\sqrt{k_\mathrm{B}T/m}$, respectively. The error bars of the simulation results are estimated from three independent runs.

Analytical results are calculated from Eqs. (23) and (17) together with Eq. (34), or from Eqs. (35)–(37), and show

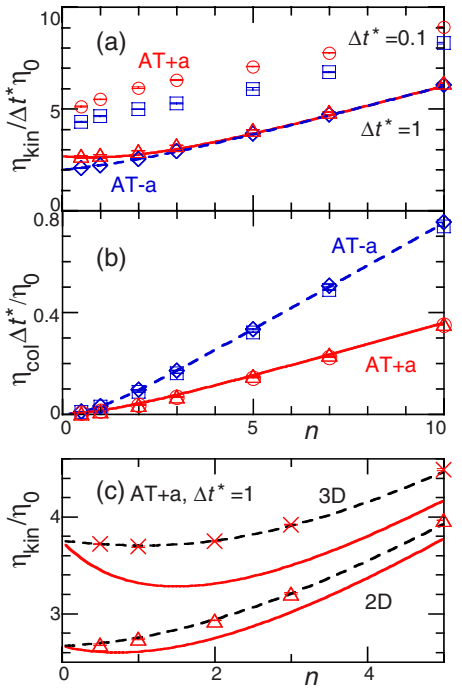

FIG. 4. (Color online) Dependence in MPC-AT $\pm a$ of the viscosities on the particle number per cell, n. (a),(c) $\eta_{\rm kin}$ and (b) $\eta_{\rm col}$. Symbols represent the numerical data of MPC-AT+a (○, △) and MPC-AT−a (□, ◇) for $\Delta t^*=0.1$ and $\Delta t^*=1$ in two dimensions, respectively, and the numerical data of MPC-AT+a at $\Delta t^*=1$ (×) in two dimensions. In (a),(b), the viscosity is rescaled by Δt^* and $1/\Delta t^*$, respectively, in order to facilitate a presentation of data for different Δt^* on the same scale. Solid and dashed lines in (a) and (b) represent analytical results for MPC-AT+a and MPC-AT−a, respectively. Solid and dashed lines in (c) represent analytical results with or without the correction term $h_{\rm m}$, respectively. Error bars are smaller than the size of symbols.

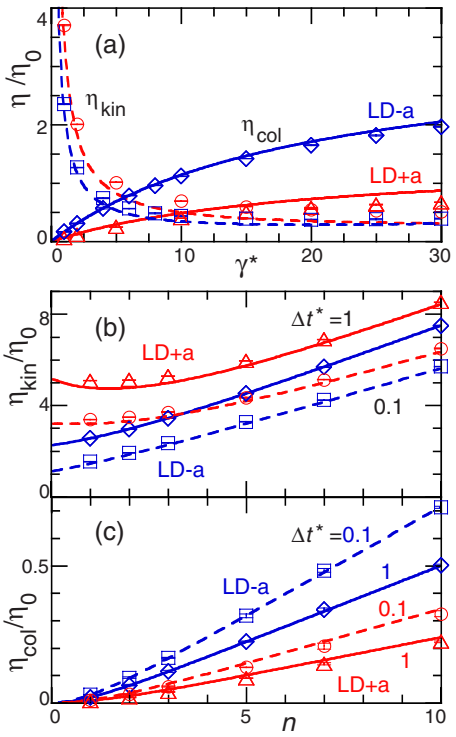

FIG. 5. (Color online) Viscosity of MPC-LD $\pm a$ as a function of (a) γ^* and (b),(c) n in three-dimensional space at (a) $n=3$ and $\Delta t^*=0.1$ and (b),(c) $\gamma^*=1$. Symbols represent the numerical data of MPC-LD+a (○, △) and MPC-LD−a (□, ◇). Dashed and solid lines represent analytical results for (a) $\eta_{\rm kin}$ or $\eta_{\rm col}$, and (b),(c) $\Delta t^*=0.1$ or 1, respectively. Error bars are smaller than the size of symbols.

generally good agreement with the numerical data, in particular for $\Delta t \simeq 1$ and large n. For smaller time step $\Delta t^*=0.1$, the most significant deviations between numerical and analytical results are found for the kinetic viscosity $\eta_{\rm kin}$, both for MPC-AT−a and MPC-AT+a, as shown in Fig. 4(a). Similar deviations between analytical and numerical results for $\eta_{\rm kin}$ have been observed for DPD in Refs. [13,21]. They have been explained by correlation effects between collisions in MPC-SR−a [30] and DPD [13]. At $\Delta t^*=0.1$, a pair of particles can collide sequentially several times; in particular for $n \lesssim 1$, pairwise collision occur frequently without involving any other particles. Thus the molecular-chaos assumption is weakly violated. There are also deviations between analytical and numerical results for the viscosity difference $\bar{\eta}_{\rm col}-\check{\eta}_{\rm col}$ of MPC−a at small Δt or small n (see Fig. 7). This is also caused by a violation of the molecular-chaos assumption.

Angular-momentum conservation does not affect the kinetic viscosity $\eta_{\rm kin}$ of MPC-AT in two dimensions at large n, compare Eqs. (19) and (28). Numerical results are shown in Figs. 3(a) and 4(a). However, the correction term in Eq. (36) predicts a small difference of $\eta_{\rm kin}$ for MPC-AT−a and MPC-AT+a for small $n \simeq 1$; see Figs. 3(b) and 4(a). The viscosities $\eta_{\rm kin}$ and $\eta_{\rm col}$ of MPC-AT−a and $\eta_{\rm col}$ of MPC-AT+a for large n show no dependence on the space dimension d (except for the scale factor $l_{\rm c}^{-d}$) therefore the corresponding lines in Fig. 3 coincide.

In two dimensions, MPC-SR with $\theta=\pi/2$ and MPC-RA with $\theta_0=\pi$ are characterized by $A=1$, and by $B=2$ and $B=1$, respectively. Thus they have the same collisional viscosity $\eta_{\rm col}$ for both their $-a$ and $+a$ version, but a different kinetic viscosity $\eta_{\rm kin}$; see Fig. 6. Although MPC-DR has the same viscosity of MPC-RA+a theoretically, the numerical data of MPC-DR shown in Fig. 3 display a slightly larger deviation from the theoretical results for $\eta_{\rm col}$ and a smaller deviation for $\eta_{\rm kin}$ than the data of MPC-RA+a.

Equation (17), together with Eq. (36), predicts a minimum of $\eta_{\rm kin}$ around $n=1$, as shown in Figs. 4(c) and 5(b). However, this minimum is not seen in numerical data and could be caused by the negligence of higher-order terms in Eq. (27). We therefore investigate the dependence of the next-order term $h/N_{\rm c}^2$, where h is a free parameter. The average is estimated by $h_{\rm m}=\Sigma_{k=3}^{\infty}P(k)h/kn \simeq \{1-e^{-n}(1+n+n^2+n^3/6-n^4/72)\}h/n^2$, which yields the asymptotic dependence $h_{\rm m}=hn^2/18$ for small n and $h_{\rm m}=h/n^2$ for $n\to\infty$. The correction term $h_{\rm m}$ is then added to Eq. (36) with h as a fit parameter. Figure 4(c) shows that this correction term with $h=-0.6$ in two dimensions and $h=-1$ in three dimensions removes the minimum and gives better agreement with the numerical data of MPC-AT+a.

Figure 8 shows the self-diffusion constant D of MPC-AT $\pm a$. The $+a$ fluid displays faster diffusion than the

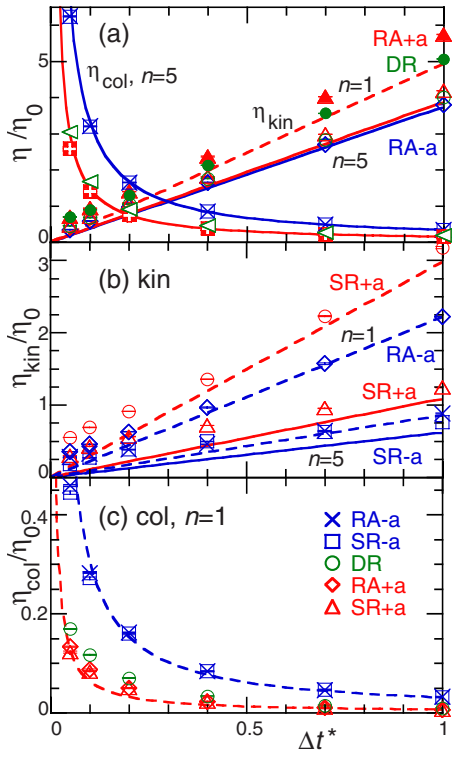

FIG. 6. (Color online) Viscosity η in two-dimensional space as a function of Δt^* for MPC-SR$\pm a$ with $\theta=\pi/2$, MPC-RA$\pm a$ with $\theta_0=\pi$, and MPC-DR with $n=1$ or $n=5$. Solid and dashed lines represent analytical results for $n=5$ and $n=1$, respectively. (a) Symbols represent the numerical data of MPC-RA+a (▲, △,+), MPC-DR (●,○,◁), MPC-RA−a (◇,×), MPC-SR−a (□), and MPC-SR+a (■). Error bars are smaller than the size of symbols.

$-a$ fluid. The diffusion constant D is numerically calculated from the mean square displacement of a particle, $\langle\{\mathbf{r}_i(t)-\mathbf{r}_i(0)\}^2\rangle=2dDt$, in a cubic simulation box with side length $L=20l_c$. Deviations from the analytical results calculated with the molecular-chaos assumption are seen for small Δt^*.

III. DISSIPATIVE PARTICLE DYNAMICS (DPD)

A. Simulation method

The DPD thermostat is a modified Langevin thermostat, where friction and noise forces are applied to the relative

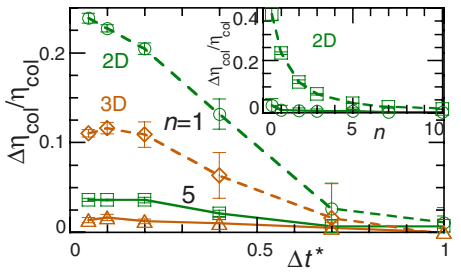

FIG. 7. (Color online) Viscosity difference $\Delta\eta_{col}=\bar{\eta}_{col}-\check{\eta}_{col}$ of MPC-AT−a in two and three dimensions. Symbols with dashed or solid lines represent the numerical data in two dimensions (○,□) and three dimensions (◇, △) at $n=1$ or $n=5$, respectively. The inset shows the dependence of $\Delta\eta_{col}$ on the average particle number n per cell, for $\Delta t^*=0.1$ (□) and $\Delta t^*=1$ (○).

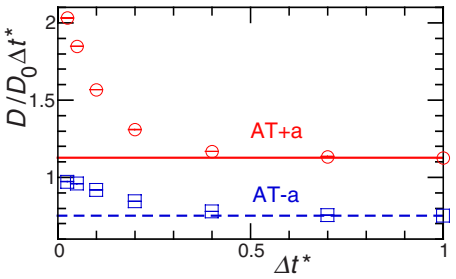

FIG. 8. (Color online) Dependence of the diffusion constant D of MPC-AT$\pm a$ on Δt at $n=5$ in three dimensions. Symbols and lines represent numerical and analytical data, respectively. Error bars are smaller than the size of symbols.

velocities of pairs of neighboring particles [5–7]. The equation of motion for the ith particle with mass m is given by

$$m\frac{d\mathbf{v}_i}{dt}=-\frac{\partial U}{\partial \mathbf{r}_i}+\sum_{j\neq i}\{-w_{ij}\mathbf{v}_{ij}\cdot\hat{\mathbf{r}}_{ij}+\sqrt{w_{ij}}\xi_{ij}(t)\}\hat{\mathbf{r}}_{ij}, \quad (38)$$

where $\mathbf{v}_{ij}=\mathbf{v}_i-\mathbf{v}_j$, $\mathbf{r}_{ij}=\mathbf{r}_i-\mathbf{r}_j$, and $\hat{\mathbf{r}}_{ij}=\mathbf{r}_{ij}/r_{ij}$, with weight $w_{ij}=w(r_{ij})$. The Gaussian white noise $\xi_{ij}(t)$ obeys the fluctuation-dissipation theorem, with $\langle\xi_{ij}(t)\rangle=0$ and $\langle\xi_{ij}(t)\xi_{i'j'}(t')\rangle=2k_BT(\delta_{ii'}\delta_{jj'}+\delta_{ij'}\delta_{ij'})\delta(t-t')$. This thermostat is applied only in the direction $\hat{\mathbf{r}}_{ij}$ to conserve the angular momentum. We denote this original method here DPD+a.

In DPD, a linear weight function $w_{ij}=w_1(r_{ij})=\gamma(1-r_{ij}/r_{cut})$ or quadratic function $w_2(r_{ij})=\gamma(1-r_{ij}/r_{cut})^2$ is typically employed, which vanishes beyond the cutoff distance $r_{ij}=r_{cut}$. Furthermore, DPD is usually combined with a soft repulsive potential U; however, we only consider the ideal-gas equation state (with potential $U=0$) in this paper.

The DPD equation (38) is discretized by the Shardlow's $S1$ splitting algorithm [9], where each thermostat of the ij pair is integrated separately,

$$\mathbf{v}_i^{new}=\mathbf{v}_i+\{-a_{dp}(r_{ij})\mathbf{v}_{ij}\cdot\hat{\mathbf{r}}_{ij}+b_{dp}(r_{ij})\xi_{ij,n}\}\hat{\mathbf{r}}_{ij},$$

$$\mathbf{v}_j^{new}=\mathbf{v}_j-\{-a_{dp}(r_{ij})\mathbf{v}_{ij}\cdot\hat{\mathbf{r}}_{ij}+b_{dp}(r_{ij})\xi_{ij,n}\}\hat{\mathbf{r}}_{ij}, \quad (39)$$

with

$$a_{dp}(r_{ij})=\frac{w_{ij}\Delta t/m}{1+w_{ij}\Delta t/m},\quad b_{dp}(r_{ij})=\frac{\sqrt{w_{ij}\Delta t}/m}{1+w_{ij}\Delta t/m}. \quad (40)$$

The discretized Gaussian noise $\xi_{ij,n}$ is determined by the variance $\langle\xi_{ij,n}\xi_{i'j',n'}\rangle=2k_BT(\delta_{ii'}\delta_{jj'}+\delta_{ij'}\delta_{ij'})\delta_{nn'}$. This splitting algorithm belongs to the class of generalized Lowe-Anderson thermostats [10], because the factors $a_{dp}(r_{ij})$ and $b_{dp}(r_{ij})$ satisfy the relation $b_{dp}=\sqrt{a_{dp}(1-a_{dp})/m}$ [20].

DPD can be modified to remove angular-momentum conservation. We denoted this technique here DPD−a. It has been introduced in Ref. [20] to explore the similarities and differences between DPD and MPC methods. In this case, the equation of motion reads [20]

$$m\frac{d\mathbf{v}_i}{dt} = -\frac{\partial U}{\partial \mathbf{r}_i} + \sum_{j\neq i}\{-w_{ij}\mathbf{v}_{ij} + \sqrt{w_{ij}}\boldsymbol{\xi}_{ij}(t)\}. \tag{41}$$

The splitting algorithm can also be applied to DPD$-a$ as $\mathbf{v}_i^{\text{new}} = \mathbf{v}_i - a_{\text{dp}}(r_{ij})\mathbf{v}_{ij} + b_{\text{dp}}(r_{ij})\boldsymbol{\xi}_{ij,n}$.

The combination of DPD$+a$ and DPD$-a$, denoted "transverse DPD," with an equation of motion determined by the difference of the right-hand sides of Eqs. (41) and (38), has been suggested very recently [50]. A similar anisotropic friction has been used in the standard Langevin equation to treat polymer entanglement implicitly in polymer melts [51] and dilute polymer solutions [52].

The DPD thermostat can be generalized into a multibody thermostat (denoted DPD-MT$-a$) [20], which is defined by the equation of motion

$$m\frac{d\mathbf{v}_i}{dt} = -\frac{\partial U}{\partial \mathbf{r}_i} - w_i^0(\mathbf{v}_i - \mathbf{v}_i^{\text{G}}) + \sqrt{w_i^0}\boldsymbol{\xi}_i(t) + \sum_{j\neq i} w_{ij}\left\{(\mathbf{v}_j - \mathbf{v}_j^{\text{G}}) - \frac{\boldsymbol{\xi}_j(t)}{\sqrt{w_j^0}}\right\}, \tag{42}$$

where $w_i^0 = \Sigma_{j\neq i} w_{ij}$, and $\mathbf{v}_i^{\text{G}} = \Sigma_{j\neq i} w_{ij}\mathbf{v}_j / w_i^0$ is the weighted mean velocity. The second term on the right-hand side of Eq. (42) is the friction term between the ith particle and its neighbors, and $N_{\text{nb}}/2$ thermostats in Eq. (41) are unified into a single thermostat, where N_{nb} is the average number of the neighbors with $r_{ij} < r_{\text{cut}}$. The third and fourth terms on the right-hand side of Eq. (42) are needed to conserve the translational momentum.

Angular momentum can be conserved in DPD-MT, when the thermostat for the ith particle is applied only in the direction $\mathbf{r}_{i,\text{G}} = \mathbf{r}_i - \mathbf{r}_i^{\text{G}}$, where the weighted center of mass is $\mathbf{r}_i^{\text{G}} = \Sigma_{j\neq i} w_{ij}\mathbf{r}_j / w_i^0$. The equation of motion of DPD-MT$+a$ is thus given by

$$m\frac{d\mathbf{v}_i}{dt} = -\frac{\partial U}{\partial \mathbf{r}_i} + \{-w_i^0(\mathbf{v}_i - \mathbf{v}_i^{\text{G}})\cdot\hat{\mathbf{r}}_{i\text{G}} + \sqrt{w_i^0}\xi_i(t)\}\hat{\mathbf{r}}_{i\text{G}} + \sum_{j\neq i} w_{ij}\left\{(\mathbf{v}_j - \mathbf{v}_j^{\text{G}})\cdot\hat{\mathbf{r}}_{j\text{G}} - \frac{\xi_j(t)}{\sqrt{w_j^0}}\right\}\hat{\mathbf{r}}_{j\text{G}}. \tag{43}$$

Shardlow's $S1$ splitting algorithm [9] can be applied to both DPD-MT$-a$ and DPD-MT$+a$. Equation (42) of DPD-MT$-a$ is discretized such that each thermostat of the i, i^{G} pair is integrated separately,

$$\mathbf{v}_i^{\text{new}} = \mathbf{v}_i - a_i^{\text{mt}}(\mathbf{v}_i - \mathbf{v}_i^{\text{G}}) + b_i^{\text{mt}}\boldsymbol{\xi}_{i,n},$$

$$\mathbf{v}_j^{\text{new}} = \mathbf{v}_j + \frac{w_{ij}}{w_i^0}\{a_i^{\text{mt}}(\mathbf{v}_i - \mathbf{v}_i^{\text{G}}) - b_i^{\text{mt}}\boldsymbol{\xi}_{i,n}\}. \tag{44}$$

The factors a_i^{mt} and b_i^{mt} are given by

$$a_i^{\text{mt}} = \frac{w_i^0\Delta t/m}{1 + \nu_i w_i^0\Delta t/2m}, \quad b_i^{\text{mt}} = \frac{\sqrt{w_i^0\Delta t}/m}{1 + \nu_i w_i^0\Delta t/2m}, \tag{45}$$

where $\nu_i = 1 + \Sigma_{j\neq i} w_{ij}^2/(w_i^0)^2$.

B. Transport coefficients

We now derive analytical expressions for the viscosity η and self-diffusion constant D of DPD$-a$ and DPD-MT$\pm a$ with ideal-gas equation of state (with potential $U=0$). The corresponding derivations for DPD$+a$ [21] can be straightforwardly carried over to this case.

The correlations of DPD$\pm a$ result from a multitude of pairwise collisions, so that $1-s_{\text{m}} = \langle\Pi_j s_{ij}\rangle$ and $1-c_{\text{m}} = \langle\Pi_j c_{ij}\rangle$. Equation (39) together with a molecular-chaos assumption implies $s_{ij} = 1 - a_{\text{dp}}\hat{x}_{ij}^2$, $c_{ij} = 1 - a_{\text{dp}}(\hat{x}_{ij}^2 + \hat{y}_{ij}^2) + 4a_{\text{dp}}^2\hat{x}_{ij}^2\hat{y}_{ij}^2$ for DPD$+a$, and $s_{ij} = 1 - a_{\text{dp}}$, $c_{ij} = 1 - 2a_{\text{dp}} + 2a_{\text{dp}}^2$ for DPD$-a$. For an ideal gas, the number of particles k per volume ΔV is given by the Poisson distribution, $P(k) = e^{-n\Delta V}(n\Delta V)^k/k!$, so that $\langle c^k\rangle = \exp\{(-1+c)n\Delta V\}$ for some constant c. This implies $1 - s_{\text{m}} = \exp(-1 + \Sigma_j\langle s_{ij}\rangle)$.

The collisional stress σ_{xy}^{col} is the momentum flux due to DPD collisions crossing a plane at $y = y_0$. After interchange of the order of integration, σ_{xy}^{col} is given by

$$\sigma_{xy}^{\text{col}} = -\frac{mn^2}{2\Delta t}\int d\mathbf{r}_{ij}(v_{i,x}^{\text{new}} - v_{i,x})y_{ij}, \tag{46}$$

where Eq. (39) and $\langle v_{ij,x}\rangle = \dot{\gamma}y_{ij}$ have been used. Thus the diffusion constant and viscosity of DPD$+a$ are given by Eq. (17) with [21]

$$D = \frac{k_{\text{B}}T\Delta t}{m}\left(\frac{1}{1 - \exp\{-n[a_{\text{dp}}(r)]_g/d\}} - \frac{1}{2}\right), \tag{47}$$

$$c_{\text{m}} = 1 - \exp\left\{n\left[-\frac{2a_{\text{dp}}(r)}{d} + \frac{4a_{\text{dp}}(r)^2}{d(d+2)}\right]_g\right\}, \tag{48}$$

$$\eta_{\text{col}} = \frac{n^2}{2d(d+2)}\left[\frac{wr^2}{1 + w\Delta t/m}\right]_g, \tag{49}$$

$$[w]_g \equiv \int g(r)w(r)dV. \tag{50}$$

In the limit $\Delta t \ll 1$, our results agree with those of the Chapman-Enskog expansion in Ref. [12]. Similarly, for DPD$-a$, D, c_{m}, and η_{col} are found to be

$$D = \frac{k_{\text{B}}T\Delta t}{m}\left(\frac{1}{1 - \exp\{-n[a_{\text{dp}}(r)]_g\}} - \frac{1}{2}\right), \tag{51}$$

$$c_{\text{m}} = 1 - \exp\{2n[-a_{\text{dp}}(r) + a_{\text{dp}}(r)^2]_g\}, \tag{52}$$

$$\eta_{\text{col}} = \frac{n^2}{2d}\left[\frac{wr^2}{1 + w\Delta t/m}\right]_g. \tag{53}$$

The only differences between the expressions for D, c_m, and η_{col} in DPD$+a$ and DPD$-a$ are prefactors containing d and $d+2$.

To simplify the equations of DPD-MT, the factors a_i^{mt} and ν_i are pre-averaged as

$$a_{\text{m}} = \frac{n[w]_g\Delta t/m}{1 + \nu_{\text{m}}n[w]_g\Delta t/2m}, \quad \nu_{\text{m}} = 1 + \frac{[w^2]_g}{n[w]_g^2}. \tag{54}$$

Then D, c_{m}, and η_{col} of DPD-MT$+a$ are given by

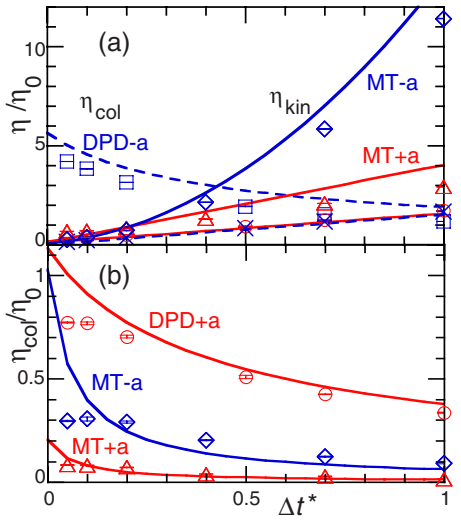

FIG. 9. (Color online) Dependence of the viscosity η on Δt^* of DPD $\pm a$ and DPD-MT $\pm a$ in three-dimensional space for $nr_{\rm cut}^3=3$ and $\gamma\tau_0/m=9$. Symbols represent the numerical data of DPD+a (○), DPD−a (×,□), DPD-MT+a (△), and DPD−a (◇). Dashed and solid lines represent analytical results for DPD−a and other DPD methods, respectively. Error bars are smaller than the size of symbols.

$$D=\frac{k_{\rm B}T\Delta t}{m}\left\{\frac{1}{1-\exp(-\nu_{\rm m}a_{\rm m}/d)}-\frac{1}{2}\right\}, \tag{55}$$

$$c_{\rm m}=1-\exp\left\{-\frac{2a_{\rm m}\nu_{\rm m}}{d}+\frac{2a_{\rm m}^2\nu_{\rm m}^2}{d(d+2)}\right\}, \tag{56}$$

$$\eta_{\rm col}=\frac{n[w^2r^2]_g}{d(d+2)[w]_g(1+\nu_{\rm m}n[w]_g\Delta t/2m)}. \tag{57}$$

Finally, for DPD-MT−a, we find

$$D=\frac{k_{\rm B}T\Delta t}{m}\left\{\frac{1}{1-\exp(-\nu_{\rm m}a_{\rm m})}-\frac{1}{2}\right\}, \tag{58}$$

$$c_{\rm m}=1-\exp(-2a_{\rm m}\nu_{\rm m}+a_{\rm m}^2\nu_{\rm m}^2), \tag{59}$$

$$\eta_{\rm col}=\frac{n[w^2r^2]_g}{d[w]_g(1+\nu_{\rm m}n[w]_g\Delta t/2m)}. \tag{60}$$

C. Numerical results

Figure 9 shows the viscosity of various DPD fluids with an ideal-gas equation of state and the linear weight $w_1(r_{ij})$. The viscosity and time step are normalized by $\eta_0=\sqrt{mk_{\rm B}T}/r_{\rm cut}^{d-1}$ and $\tau_0=r_{\rm cut}\sqrt{m/k_{\rm B}T}$, respectively. The dimensionless time step is $\Delta t^*=\Delta t/\tau_0$, as before. There is in general good agreement between analytical and numerical results. However, small deviations are visible. One reason for these deviations is that the molecular-chaos assumption is not perfectly valid [13]. In the case of DPD-MT $\pm a$, another reason is the pre-averaging procedure used in the derivation of the analytical expressions, which neglects some correlations.

The kinetic (collisional) viscosities of DPD+a and DPD-MT+a are larger (smaller) than those of the −a versions, since angular-momentum conservation reduces the momentum transfer in DPD collisions. A similar behavior has also been found for MPC $\pm a$ in Sec. II.

IV. THERMOSTATING MESOSCALE FLUIDS UNDER FLOW

In experiments, systems are usually thermostated on their boundaries. However, in simulations, thermostats typically act on all fluid particles in order to avoid temperature gradients. In flows, the temperature is defined under the assumption of local equilibrium. In the MPC and DPD families, the length scales which define this "local" environment are $l_{\rm c}$ and $r_{\rm cut}$, respectively. On these scales, the thermal fluctuations should be separated from the macroscopic flow, and the thermostats should act on the local kinetic energy to fix the temperature.

The conditions on the shear rate $\dot\gamma$ for this local equilibrium to hold are obtained as follows. All of thermostats of the MPC family are profile-unbiased thermostats (PUT) [45]. Thus the condition for a maximum shear rate of PUT [53] also apply to MPC. In simple shear flow with low Reynolds number, the particle velocities are characterized by $\langle\mathbf{v}_i(\mathbf{r}_i)\rangle=\dot\gamma y_i\mathbf{e}_x$ and $\langle\mathbf{v}_i(\mathbf{r}_i)^2\rangle=dk_{\rm B}T/m+\dot\gamma^2y_i^2$. In MPC, the particle velocity $\mathbf{v}_{i,{\rm c}}$ relative to the center-of-mass velocity of a MPC collision cell is employed to calculate the kinetic energy in the local rest frame,

$$\frac{1}{N_{\rm c}-1}\sum_{i\in{\rm cell}}\langle\mathbf{v}_{i,{\rm c}}^2\rangle=\frac{dk_{\rm B}T}{m}+\frac{\dot\gamma^2l_{\rm c}^2}{12}, \tag{61}$$

where the average is taken over all particles in a cell. For $\dot\gamma l_{\rm c}\ll\sqrt{k_{\rm B}T/m}$, the second term in Eq. (61) is negligible, and the thermal fluctuations and shear are well separated. On the other hand, for $\dot\gamma l_{\rm c}\gtrsim\sqrt{k_{\rm B}T/m}$, the thermostats couple with the macroscopic flow and may modify the flow behavior.

In DPD+a, the relative velocity $\mathbf{v}_{ij}$ of neighboring particles is employed instead,

$$\langle(\mathbf{v}_{ij}\cdot\hat{\mathbf{r}}_{ij})^2\rangle=\frac{2k_{\rm B}T}{m}+\frac{[(\dot\gamma r\hat x\hat y)^2w]_g}{[w]_g}. \tag{62}$$

For the linear weight $w_1(r_{ij})$ and uniform radial distribution function $g(r)$, the second term in Eq. (62) is $\{(d+1)/(d+2)^2(d+3)\}(\dot\gamma r_{\rm cut})^2$. Thus the condition for thermostats to provide local equilibrium conditions is $\dot\gamma r_{\rm cut}\ll\sqrt{k_{\rm B}T/m}$.

To study the hydrodynamic behavior of complex fluids, the parameter ranges of simulations should of course also match physical conditions of experiments. Thus the simulation parameters have to be chosen such as to adjust dimensionless hydrodynamic quantities, like the Reynolds number, the Schmidt number, and the Knudsen number.

V. SUMMARY

MPC and DPD are very versatile simulation techniques for mesoscale hydrodynamics. By employing different types of collision rules and thermostats, it is possible to construct a

variety of algorithms with different properties. One of the important properties is whether an algorithm does or does not conserve angular momentum. The angular momentum conservation can be switched on or off in each variant of MPC and DPD.

In addition to previous MPC algorithms, we have introduced here MPC-SR+a. This algorithm has to be used with some caution, because compared to other MPC+a techniques, it does not give a uniform radial distribution function. However, the deviations are small for sufficiently large density and not too small time step.

We have derived analytical expressions for the viscosity η and the self-diffusion constant D of various MPC and DPD methods. The theoretical results show very good agreement with numerical results. Since we provide very general expressions of η and D for MPC, the transport coefficients of any new version of MPC can now be obtained very easily by calculating the two correlation factors A and B (compare Table I). Many similarities between MPC and DPD are seen in the derivation of η and D and the relation between the $-a$ and $+a$ versions. We believe that these similarities apply generally for particle-based hydrodynamics methods.

ACKNOWLEDGMENTS

We thank T. Ihle (North Dakota State University) and I. O. Götze for helpful discussions. Support of this work by the DFG through the SFB TR6, "Physics of Colloidal Dispersions in External Fields," is acknowledged.

[1] *Molecular Gas Dynamics*, edited by G. A. Bird (Clarendon, Oxford, 1976).
[2] G. A. Bird, Comput. Math. Appl. **35**, 1 (1998).
[3] S. Succi, *The Lattice Boltzmann Equation: For Fluid Dynamics and Beyond* (Oxford University Press, Oxford, 2001).
[4] J. M. Yeomans, Physica A **369**, 159 (2006).
[5] P. J. Hoogerbrugge and J. M. V. A. Koelman, Europhys. Lett. **19**, 155 (1992).
[6] R. D. Groot and P. B. Warren, J. Chem. Phys. **107**, 4423 (1997).
[7] P. Español, Phys. Rev. E **57**, 2930 (1998).
[8] I. Pagonabarraga, M. H. J. Hagen, and D. Frenkel, Europhys. Lett. **42**, 377 (1998).
[9] T. Shardlow, SIAM J. Sci. Comput. (USA) **24**, 1267 (2003).
[10] E. A. J. F. Peters, Europhys. Lett. **66**, 311 (2004).
[11] M. P. Allen, J. Phys. Chem. B **110**, 3823 (2006).
[12] C. A. Marsh, G. Backx, and M. H. Ernst, Phys. Rev. E **56**, 1676 (1997).
[13] A. J. Masters and P. B. Warren, Europhys. Lett. **48**, 1 (1999).
[14] M. Ripoll, M. H. Ernst, and P. Español, J. Chem. Phys. **115**, 7271 (2001).
[15] E. S. Boek, P. V. Coveney, H. N. W. Lekkerkerker, and P. van der Schoot, Phys. Rev. E **55**, 3124 (1997).
[16] N. A. Spenley, Europhys. Lett. **49**, 534 (2000).
[17] P. Nikunen, I. Vattulainen, and M. Karttunen, Phys. Rev. E **75**, 036713 (2007).
[18] M. Venturoli, M. M. Sperotto, M. Kranenburg, and B. Smit, Phys. Rep. **437**, 1 (2006).
[19] A. Grafmüller, J. Shillcock, and R. Lipowsky, Phys. Rev. Lett. **98**, 218101 (2007).
[20] H. Noguchi, N. Kikuchi, and G. Gompper, Europhys. Lett. **78**, 10005 (2007).
[21] H. Noguchi and G. Gompper, Europhys. Lett. **78**, 36002 (2007).
[22] A. Malevanets and R. Kapral, J. Chem. Phys. **110**, 8605 (1999).
[23] T. Ihle and D. M. Kroll, Phys. Rev. E **63**, 020201(R) (2001).
[24] A. Lamura, G. Gompper, T. Ihle, and D. M. Kroll, Europhys. Lett. **56**, 319 (2001).
[25] E. Allahyarov and G. Gompper, Phys. Rev. E **66**, 036702 (2002).
[26] N. Kikuchi, C. M. Pooley, J. F. Ryder, and J. M. Yeomans, J. Chem. Phys. **119**, 6388 (2003).
[27] C. M. Pooley and J. M. Yeomans, J. Phys. Chem. B **109**, 6505 (2005).
[28] T. Ihle and D. M. Kroll, Phys. Rev. E **67**, 066706 (2003).
[29] T. Ihle, E. Tüzel, and D. M. Kroll, Phys. Rev. E **72**, 046707 (2005).
[30] E. Tüzel, T. Ihle, and D. M. Kroll, Phys. Rev. E **74**, 056702 (2006).
[31] J. T. Padding and A. A. Louis, Phys. Rev. Lett. **93**, 220601 (2004).
[32] J. T. Padding and A. A. Louis, Phys. Rev. E **74**, 031402 (2006).
[33] M. Hecht, J. Harting, T. Ihle, and H. J. Herrmann, Phys. Rev. E **72**, 011408 (2005).
[34] M. Ripoll, K. Mussawisade, R. G. Winkler, and G. Gompper, Europhys. Lett. **68**, 106 (2004).
[35] M. Ripoll, R. G. Winkler, and G. Gompper, Phys. Rev. Lett. **96**, 188302 (2006).
[36] S. H. Lee and R. Kapral, J. Chem. Phys. **124**, 214901 (2006).
[37] T. Sakai, Y. Chen, and H. Ohashi, Phys. Rev. E **65**, 031503 (2002).
[38] H. Noguchi and G. Gompper, Phys. Rev. Lett. **93**, 258102 (2004).
[39] H. Noguchi and G. Gompper, Proc. Natl. Acad. Sci. U.S.A. **102**, 14159 (2005).
[40] H. Noguchi and G. Gompper, J. Chem. Phys. **125**, 164908 (2006).
[41] T. Ihle, E. Tüzel, and D. M. Kroll, Europhys. Lett. **73**, 664 (2006).
[42] G. Rückner and R. Kapral, Phys. Rev. Lett. **98**, 150603 (2007).
[43] I. O. Götze, H. Noguchi, and G. Gompper, Phys. Rev. E **76**, 046705 (2007).
[44] G. Gompper, T. Ihle, D. M. Kroll, and R. G. Winkler, Adv. Polym. Sci. (to be published).
[45] D. J. Evans and G. P. Morriss, Phys. Rev. Lett. **56**, 2172 (1986).
[46] M. P. Allen and D. J. Tildesley, *Computer Simulation of Liq-*

uids (Clarendon Press, Oxford, 1987).
[47] H. C. Andersen, J. Chem. Phys. **72**, 2384 (1980).
[48] J. F. Ryder, Ph.D. thesis, University of Oxford, 2005.
[49] L. D. Landau and E. M. Lifshitz, *Fluid Mechanics*, 2nd ed. (Pergamon Press, Oxford, 1987).
[50] C. Junghans, M. Praprotnik, and K. Kremer, Soft Matter **4**, 156 (2008).
[51] R. B. Bird, C. F. Curtiss, R. C. Armstrong, and O. Hassager, *Dynamics of Polymeric Liquids* (Wiley, New York, 1987), Vol. 2.
[52] H. Noguchi, J. Chem. Phys. **112**, 9671 (2000).
[53] W. Loose and G. Ciccotti, Phys. Rev. A **45**, 3859 (1992).